

# Preparation of high-sensitivity $\text{In}_2\text{S}_3/\text{Si}$ heterojunction photodetector by chemical spray pyrolysis

Raid A. Ismail<sup>1</sup> · Nadir F. Habubi<sup>2</sup> · Mahmood M. Abbod<sup>2</sup>

Received: 3 June 2016 / Accepted: 3 September 2016 / Published online: 9 September 2016  
© Springer Science+Business Media New York 2016

**Abstract** High photosensitivity n- $\text{In}_2\text{S}_3/\text{p-Si}$  heterojunction photodetectors were made by depositing indium sulfide  $\text{In}_2\text{S}_3$  thin film on a p-type silicon substrate using chemical spray pyrolysis with molarity of 0.1 and 0.2 M at 400 °C. Characterization techniques of X-ray diffraction XRD, scanning electron microscopy SEM, energy dispersive X-ray EDX, atomic force microscopy AFM, UV–Vis spectrophotometer, and Hall measurements were utilized to investigate structural, optical and electrical properties of the films. XRD investigation revealed polycrystalline grown films. EDX analysis showed good stoichiometry synthesized films with [S]/[In] ratios of 1.04 and 1.08 for  $\text{In}_2\text{S}_3$  films prepared with 0.1 and 0.2 M respectively. Optical energy gap of the films decreased from 2.87 to 2.7 eV after increasing film morality from 0.15 to 0.2 M. Photo-response investigation of photodetector prepared with 0.2 M showed two peaks of response located at 400 and 750 nm with photosensitivity of 0.5 and 0.68  $\text{A W}^{-1}$  respectively. Pulsed responsivity of photodetectors at 365 nm was found to be 200  $\text{mV W}^{-1}$  at 0.1 M and 250  $\text{mV W}^{-1}$  at 0.2 M.

**Keywords** Indium sulfide · Spray pyrolysis · Silicon · Heterojunction

## 1 Introduction

Indium sulfide is an interesting and promising II–VI material due to its stability, high optical transparency and conductivity (Lin et al. 2014; Kaleel et al. 2014; Kraini et al. 2013). It has direct energy gap ranging from 2 to 2.8 eV at 300 K.  $\text{In}_2\text{S}_3$  film has been used efficiently as a buffer layer for high efficiency CIGS thin film solar cells. Many methods

---

✉ Raid A. Ismail  
raidismail@yahoo.com

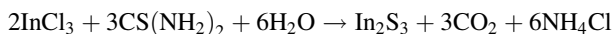
<sup>1</sup> Department of Applied Science, University of Technology, Baghdad, Iraq

<sup>2</sup> Department of Physics, Education Faculty, University of Mustansiriya, Baghdad, Iraq

have been used to prepare  $\text{In}_2\text{S}_3$  thin films, such as; chemical spray pyrolysis (Hariskos et al. 1996), chemical bath deposition (Naghavi et al. 2003), metal organic chemical vapor deposition (Lajnef and Ezzaouia 2009), and pulsed laser deposition (El Sbazly and Abd 1998), spray pyrolysis (John et al. 2006), thermal evaporation (Asikainen et al. 1994), spin coating (Warrier et al. 2009), and atomic layer deposition (Hsiao et al. 2014). Heterojunction thin films based CdS have draw attention due to their high performance particularly in the case of high efficiency solar cells and high photosensitivity photodetectors. The main drawback of using CdS is the toxicity of Cd and therefore, the development of the photovoltaic devices needs to replace this toxic metal with other environment friendly metals (Sall et al. 2014). It was reported that the Indium sulfide film is a good alternative for such use (Lajnef and Ezzaouia 2009). Fabrication of high photosensitivity and very fast silicon heterojunction photodiode by depositing of two dimensional (2D) alloys film on silicon has attracted intense attention owing to their bandgap tunability and potential optoelectronic applications (Yuan et al. 2015a, b; Liu et al. 2015). Indium sulfide film has a good transmission in the blue region with wider band gap than cadmium sulfide. Recently, Hsiao et al. (2014) prepared  $\text{In}_2\text{S}_3/\text{n-Si}$  heterojunction by hydrothermal method. Up to best of our knowledge no data have been found in literatures on preparing of  $\text{In}_2\text{S}_3/\text{Si}$  heterojunction by chemical spray pyrolysis technique. The main advantages of chemical spray pyrolysis over the others deposition methods are cost effectiveness, large area deposition, no vacuum is required, good control on deposition parameters, allow effective doping and deposition of multi-component film (Sabnis et al. 2013). In this study, preparation and characterization of high photosensitivity anisotype  $\text{In}_2\text{S}_3/\text{Si}$  heterojunction photodetector by chemical spray pyrolysis is demonstrated and analyzed.

## 2 Experimental

Indium sulfide thin films were deposited on cleaned Corning glass and mirror-like single crystal silicon substrates by chemical spray pyrolysis technique. The silicon substrates were used here were p-type of  $1 \text{ cm}^2$  area and having electrical resistivity of  $3 \Omega \text{ cm}$  and orientation of (111). The spraying solution was contained of indium chloride  $\text{InCl}_3$  (purity of 99 % provided from Thomas Baker Co.) and thiourea ( $\text{CS}(\text{NH}_2)_2$ ) dissolved in distilled water. The starting solutions were sprayed on glass and silicon substrates with molar concentrations of 0.1 and 0.2 M. Compressed air was used as gas carrier, the total volume of solution sprayed was 100 mL and the spray rate was around  $1.5 \text{ mL min}^{-1}$ . The deposition temperature was kept at  $400 \text{ }^\circ\text{C}$  with accuracy of  $\pm 5 \text{ }^\circ\text{C}$  using temperature control. The formation of  $\text{In}_2\text{S}_3$  film was established according the following chemical reaction:



The structural properties of as-grown films were characterized by X-ray diffractometer (type: Shimadzu, model: XRD6000) using  $\text{CuK}\alpha$  radiation ( $\lambda = 0.15406 \text{ nm}$ ) with scan angle of  $2\theta = 20^\circ\text{--}60^\circ$ . Scanning electron microscope (T-scan Vega III Czech) was used to investigate the surface structure of the films and the chemical composition of the films was investigated using energy dispersive X-ray EDX analysis. The thickness of the film was measured using laser interferometer. The optical properties of the films was measured using UV-Vis spectrophotometer (type: CARY, model: 100 CONC plus). AFM (AA 3000 Scanning Probe Microscope) was employed to study the surface morphology of the

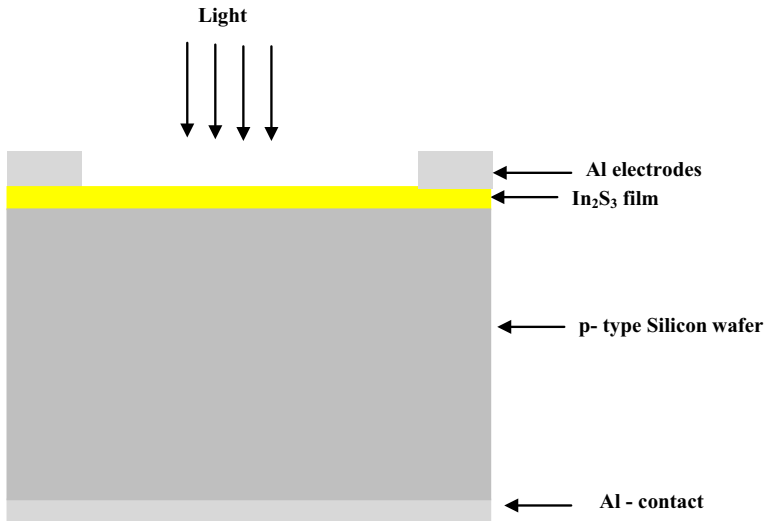
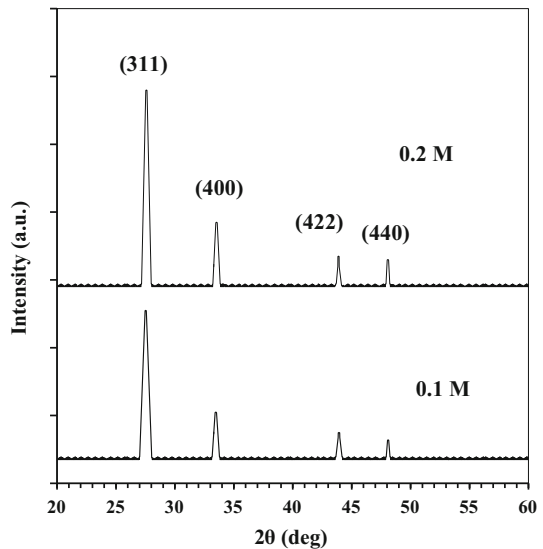


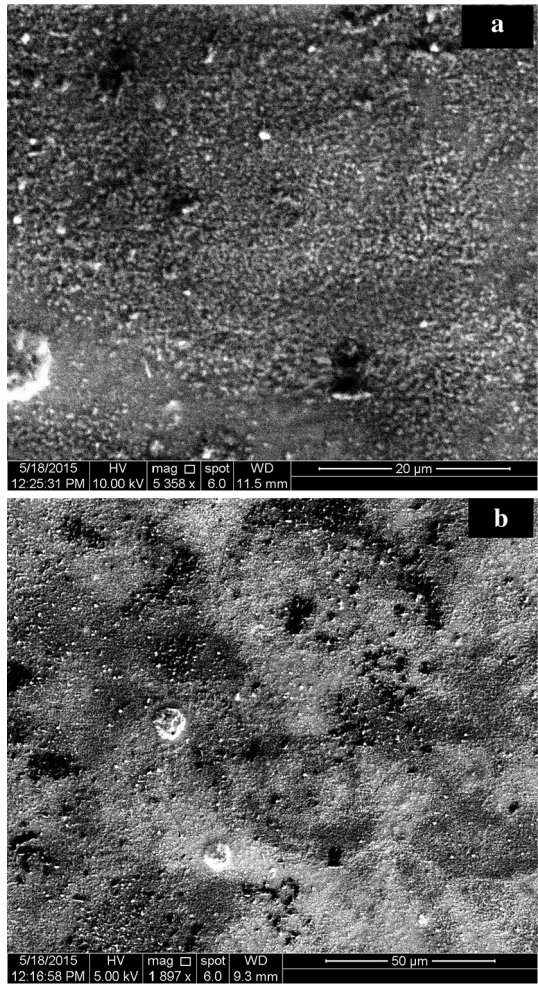
**Fig. 1** Cross-sectional diagram view of  $\text{In}_2\text{S}_3/\text{p-Si}$  heterojunction photodetector

**Fig. 2** XRD patterns of  $\text{In}_2\text{S}_3$  thin films prepared at 0.1 and 0.2 M



synthesised films. Mobility and carrier concentration of the deposited films were investigated using Hall effect (type: Ecopia, model: HMS3000). To investigate the heterojunction properties, ohmic contacts were made on  $\text{In}_2\text{S}_3$  film and back side of silicon wafer by depositing of Al electrodes (Hsiao et al. 2014) by thermal resistive technique through special designed mask. Figure 1 illustrates the schematic diagram of  $\text{In}_2\text{S}_3/\text{p-Si}$  heterojunction. Dark and illuminated I–V characteristics of  $\text{In}_2\text{S}_3/\text{Si}$  heterojunctions were measured using halogen lamp, ammeter and DC power supply. The spectral responsivity of photodetectors have been measured in the range 375–900 nm using monochromator (Jobin–Yvon) with the power being calibrated using “Sanwa” silicon power meter. The

**Fig. 3** SEM images of  $\text{In}_2\text{S}_3$  thin films with 0.1 M **a** low magnification SEM image, **b** higher magnification SEM image

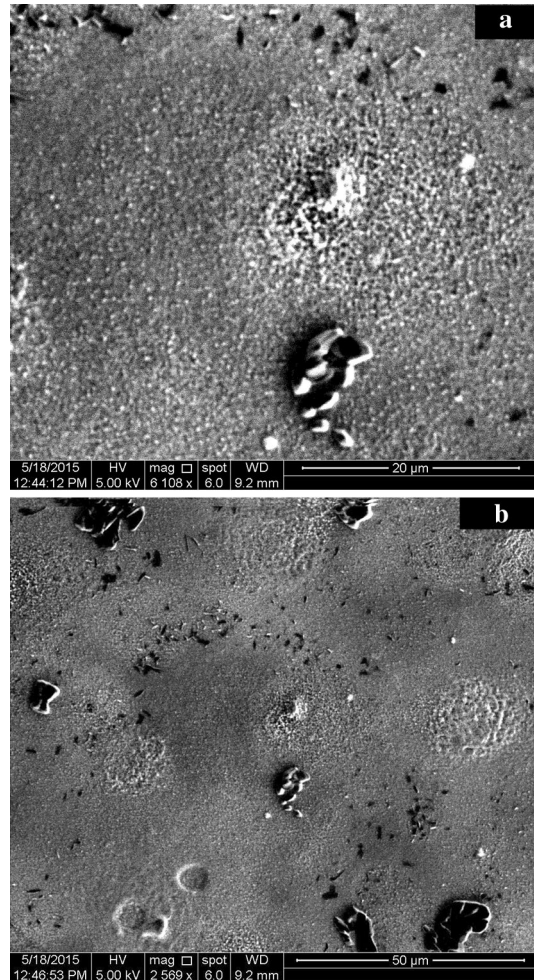


pulsed responsivity at 365 nm was investigated using UV source and 200 MHz oscilloscope.

### 3 Results and discussion

Figure 2 displays XRD patterns of 0.1 and 0.2 M indium sulfide thin films, the film was scanned in the range of  $20^\circ$ – $60^\circ$ . It is seen from this figure the films exhibits a strong peak around  $27.52^\circ$  and three weaker peaks at  $33.47^\circ$ ,  $43.92^\circ$ , and  $48.09^\circ$  corresponding to (311), (400), (422), and (440) reflecting planes, respectively. All these diffraction peaks are indexed to cubic structure of the polycrystalline  $\text{In}_2\text{S}_3$  according to ICDD card no. 32-0456 (Gopinath et al. 2013). XRD pattern shows preferred growth of crystallites along the (311) plane. Neither impurity phase nor incomplete phases were observed in the XRD patterns. The diffracted peaks intensity increases as the film molar concentration increase; an

**Fig. 4** SEM images of  $\text{In}_2\text{S}_3$  thin films with 0.2 M **a** low magnification SEM image, **b** higher magnification SEM image



indication increasing of the crystallinity degree. The lack of (220) and (511) planes refers to preferred growth direction.

The crystallite size of the synthesised films calculated for (311) plane from X-ray line broadening analysis using Scherrer's equation was found to be 11 nm for 0.1 M film and 8 nm for 0.2 M film. The morphology and particle size of synthesised indium sulfide films have been investigated using SEM. Figures 3 and 4 show SEM images of indium sulfide film sprayed at 0.1 and 0.2 M respectively. These films consist of nonuniform particles (aggregate of smaller crystallites) of approximately 0.35–1 and 0.5–1.1 µm in size for 0.1 and 0.2 M films, respectively. SEM images illustrate rougher surface at higher molar concentration (0.2 M). The sprayed films seem free of cracks or pinholes. EDX spectra given in Fig. 5 show the presence of In, S, Ca, O, N, and Cl impurities. The origin source of Ca, O, N, and Cl impurities was the glass substrate. The EDX spectra showed that the peaks of In and S have of nearly equal intensity as shown in Table 1.

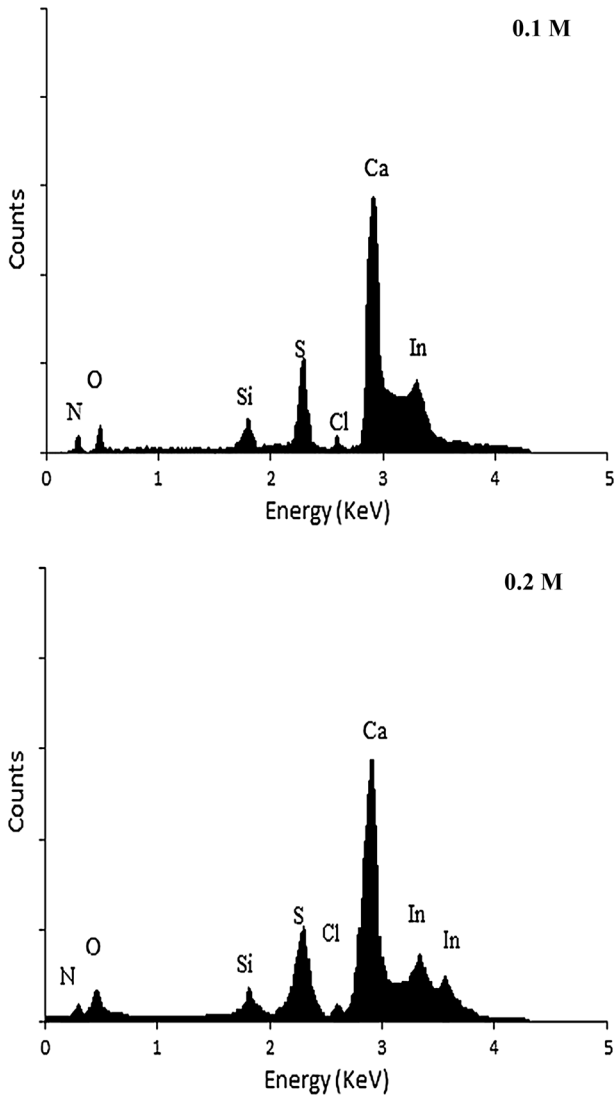


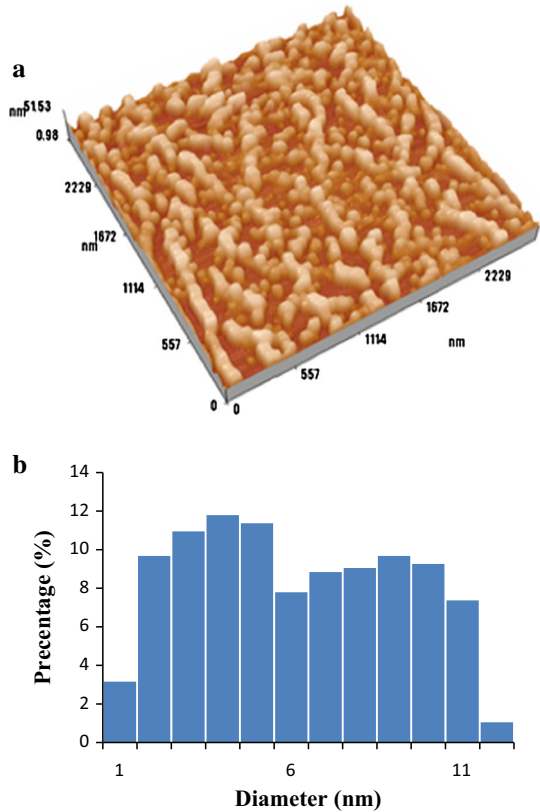
**Fig. 5** EDX spectra of  $\text{In}_2\text{S}_3$  films

**Table 1** Ratios of indium and sulfur in thin films

Element	Content%	
	At 0.1 M	At 0.2 M
In	15.36	16.01
S	16.02	17.3

From Table 1 it is clear that the measured S/In ratios were 1.04 and 1.08 for 0.1 and 0.2 M films, respectively, indicating no significant effect of molar concentration on sulfur-indium ratio. The film surface morphology was studied by AFM technique. Figures 6 and 7

**Fig. 6** 3D AFM image (a) and granularity accumulation distribution plot (b) of In<sub>2</sub>S<sub>3</sub> prepared with 0.1 M



show 3D AFM images of In<sub>2</sub>S<sub>3</sub> films synthesised with 0.1 and 0.2 M, respectively. These films were dense and consist of small ball-shaped grains with relatively uniform distribution as illustrated in Fig. 4b.

It is clearly seen film's morphology depends on molar concentration, the root mean square roughness RMS of the film increased from 5 to 7 nm as the molar concentration increased from 0.1 to 0.2 M. The average grain size of the film was estimated from AFM measurement using special software and found around 63 nm for 0.1 M film and 88 nm for 0.2 M film as shown in Table 2, these values are different from those determined from XRD and SEM investigations, and this could be caused by particles agglomeration led to the formation of clusters of different dimensions.

Figure 8 shows the optical transmittance spectra of indium sulfide films prepared with 0.1 and 0.2 M having thickness of 250 and 330 nm, respectively. The synthesized films exhibited transparency in the range 550–900 nm, the optical transmittance spectra of 250 and 330 nm indium sulfide films thick prepared with 0.1 and 0.2 M respectively. The films exhibited maximum transmission of 71 % in the range 550–900 nm; but it decreased after increasing the molar concentration from 0.1 to 0.2 M, because of increasing the film thickness and decreasing the surface roughness. The optical band gap  $E_g$  of the films was calculated from Tauc law (Tauc et al. 1966):

$$\alpha hv = A(hv - E_g)^n \quad (1)$$

**Fig. 7** 3D AFM image (a) and granularity accumulation distribution plot (b) of  $\text{In}_2\text{S}_3$  prepared with 0.2 M

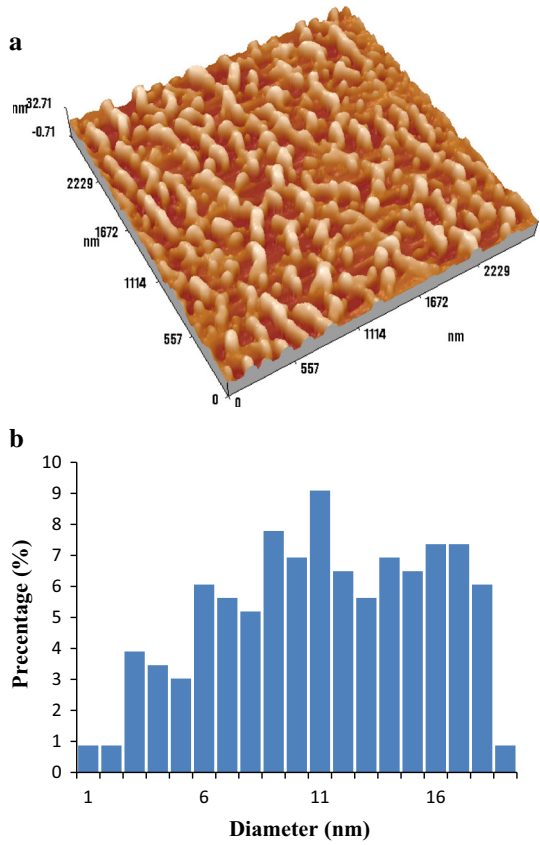


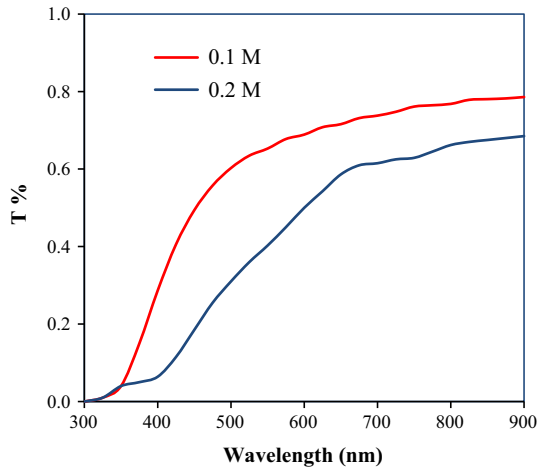
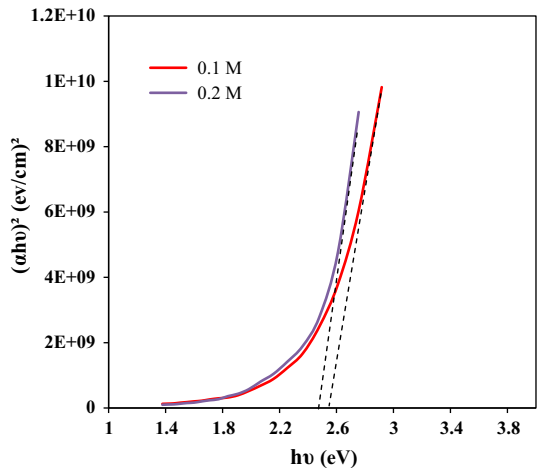
**Table 2** RMS and avg. diameter of  $\text{In}_2\text{S}_3$  thin films with different molarities

Molarity (M)	Root mean square of surface roughness (nm)	Avg. diameter (nm)
0.1	7	63
0.2	5	88

where  $\alpha$  is the film absorption coefficient,  $h\nu$  is photon energy,  $A$  is a constant,  $h$  is the Plank constant,  $n$  is the exponent that gives the type of band transition. The value of  $n$  was calculated and found to be 0.46; indicating a direct band transition. The optical energy gap was determined from the  $(\alpha h\nu)^2$  versus  $h\nu$  plot in Fig. 9 by extrapolating the straight line of the curve to the  $h\nu = 0$  points. The energy gap values of indium sulfide films sprayed at 0.1 and 0.2 M were 2.41 and 2.52 eV, respectively. These values are higher than those for bulk indium sulfide films due to the presence of an excess of sulfur in their bulk (Kim and Kim 1986). The reason of slightly increase of energy gap can be ascribed to increasing of S/In ratio which results in presence of excess sulphur and film thickness (Hsiao et al. 2014).

The estimated values of energy gap are in good agreement with those reported in literatures (Hsiao et al. 2014; Yoshida et al. 1997). Hall measurements revealed that the indium sulfide films have n-type conductivity. The electron concentration decreases from



**Fig. 8** Optical transmittance of In<sub>2</sub>S<sub>3</sub> films**Fig. 9**  $(\alpha h\nu)^2$  versus  $h\nu$  plot of In<sub>2</sub>S<sub>3</sub> thin films

$3.3 \times 10^{15}$  to  $2 \times 10^{15} \text{ cm}^{-3}$  as molar concentration increases from 0.1 to 0.2 M, while increasing the molar concentration results in increasing the electron mobility from 63 to  $120 \text{ cm}^2 \text{ V}^{-1} \text{ s}^{-1}$ . The increase of mobility with molar concentration could be linked to increasing of film' grain size, grain boundary and due the improvement in crystallinity of the film. The dark current–voltage characteristics of n-In<sub>2</sub>S<sub>3</sub>/p-Si heterojunctions is given in Fig. 10, which exhibits good rectification characteristics (well-defined diode-like behavior).

The rectification ratio of heterojunction prepared at 0.2 M is higher than that of heterojunction prepared with 0.1 M. The forward current has increased with molar concentration due to the increased conductivity of In<sub>2</sub>S<sub>3</sub> film. It was noticed that the forward I–V characteristics of synthesised heterojunctions is obey to the following (I–V) relationship (Streetman and Banerjee 2010):

$$I = I_0 \left( e^{\frac{qV}{kT}} - 1 \right) \quad (2)$$

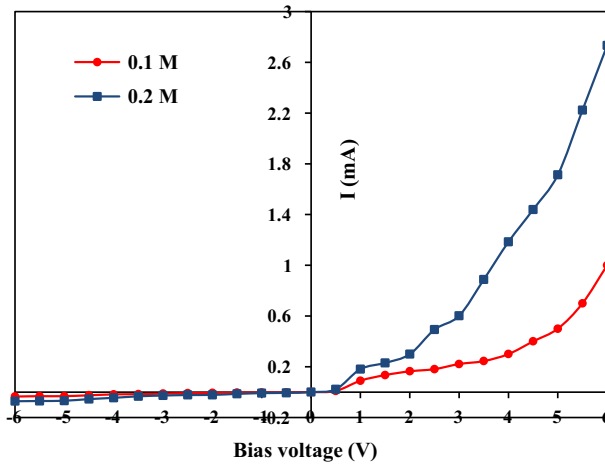


**Fig. 10** Dark I–V characteristics of the  $\text{In}_2\text{S}_3/\text{Si}$  heterojunctions

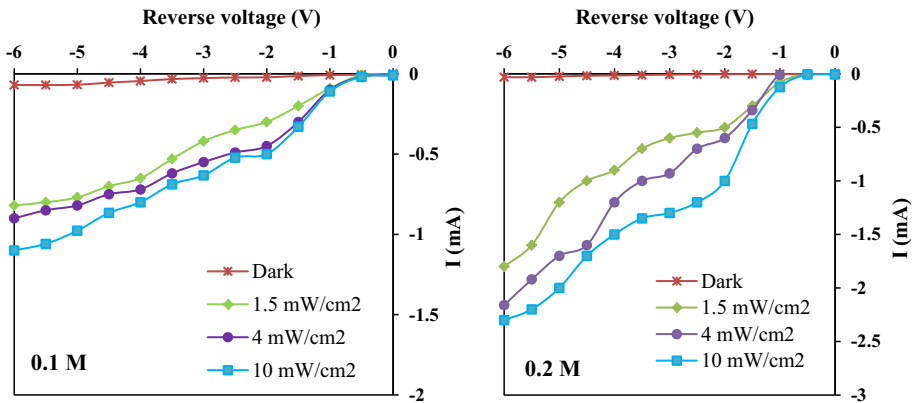


**Fig. 11** Dark and illuminated I–V characteristics of  $\text{In}_2\text{S}_3/\text{Si}$  photodetectors prepared at 0.1 and 0.2 M

where  $I_0$  is the saturation current and  $\beta$  is the diode ideality factor. The value of ideality factor  $\beta$  of heterojunctions was calculated from Eq. 2 and found to be 4 and 2.5 for heterojunctions prepared with 0.1 and 0.2 M, respectively; indicating the domination of the current transport by recombination process. The large values of  $\beta$  can originate from structural defects originated from interfacial defects, surface states and surface oxides effects, as well as the large value lattice mismatch lattice between  $\text{In}_2\text{S}_3$  and Si. This lattice mismatch between  $\text{In}_2\text{S}_3$  and Si was calculated and found to vary from 35 to 33 % as molarity increased from 0.1 to 0.2 M. The mismatch is caused by lattice strain; and the later was calculated and found to decrease from  $14.4 \times 10^{-3}$  to  $8.3 \times 10^{-3}$  as film molarity increases from 0.1 to 0.2 M. The saturation current density of heterojunction can be given by the following expression:

$$I_0 = Be^{-\frac{E_{g0}}{kT}} \tag{3}$$

**Fig. 12** Effect of film molarity on the responsivity of photodetectors

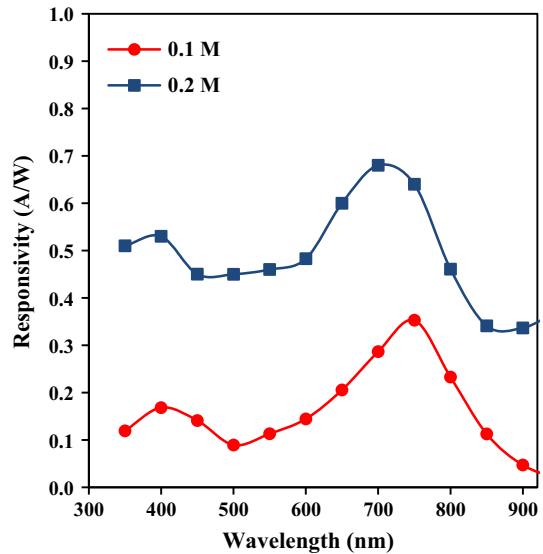
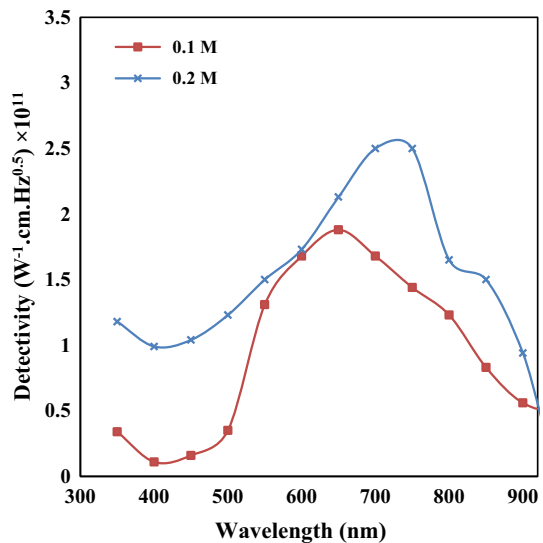


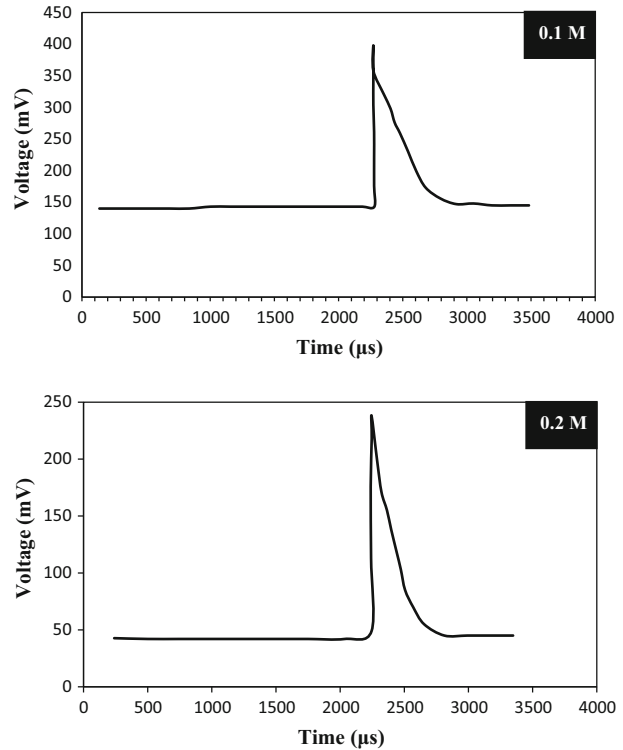
**Fig. 13** Detectivity of  $\text{In}_2\text{S}_3/\text{Si}$  photodetectors



where  $B$  is constant and  $E_{ac}$  represents the activation energy. The reverse bias leakage current of the heterojunctions is small and no breakdown was noticed at voltage up to 6 V.

The illuminated  $I-V$  characteristics of the heterojunctions under reverse direction are given in Fig. 11, which illustrates an increasing photocurrent with light intensity increase. This demonstrates good linearity of synthesised photodetectors. The values of on/off ratios for photodetectors prepared with 0.1 and 0.2 M of  $\text{In}_2\text{S}_3$  films were 15 and 88 at 5 V, respectively. The large value of on/off ratio of photodetector prepared with 0.2 M of  $\text{In}_2\text{S}_3$  film can be attributed to high crystallinity of  $\text{In}_2\text{S}_3$  film, wide band gap and large depletion layer width (Zhong et al. 2014). Figure 12 illustrates the spectral responsivity plot of  $\text{In}_2\text{S}_3/$

**Fig. 14** Open-circuit voltage decay plots for  $\text{In}_2\text{S}_3/\text{Si}$  prepared at different molarities



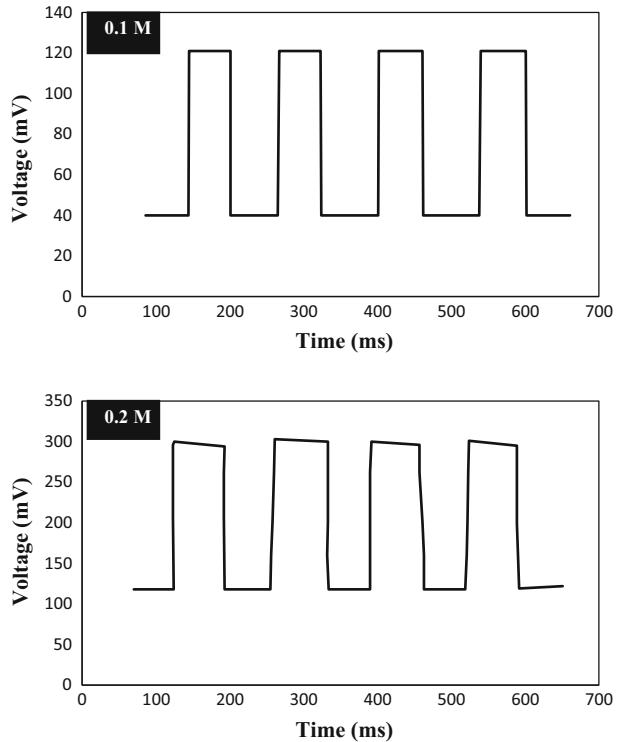
$\text{Si}$  heterojunctions prepared with 0.1 and 0.2 M at 2 V bias. Each heterojunction has two peaks of response; one around 400 nm due to absorption edge of  $\text{In}_2\text{S}_3$  film, and another around 450 nm; caused by absorption edge of silicon substrate. Increasing the molar concentration of  $\text{In}_2\text{S}_3$  film to 0.2 M resulted in a significant increase of responsivity at visible and near IR regions.

The obtained value of responsivity at visible region is higher than that those for other wide band gap based silicon heterojunctions devices (Ismail et al. 2013; Ismail 2006). Figure 13 shows the specific detectivity  $D^*$  plots for  $\text{In}_2\text{S}_3/\text{Si}$  heterojunction photodetectors biased to 2 V. The maximum detectivity was  $2.5 \times 10^{11} \text{ W}^{-1} \text{ cm Hz}^{0.5}$  at 700 nm for heterojunction prepared with 0.2 M of  $\text{In}_2\text{S}_3$  film, while the heterojunction sprayed with 0.1 M of  $\text{In}_2\text{S}_3$  has detectivity of  $1.88 \times 10^{11} \text{ W}^{-1} \text{ cm Hz}^{0.5}$  at 650 nm. The small shift in peak detectivity of photodetectors is probably due to variation the  $S/\text{In}$  ratio that affecting the energy gap of  $\text{In}_2\text{S}_3$  thin film. Open circuit voltage decay OCVD method was used to measure the photo-generated minority carrier life time MCLT ( $\tau$ ) of the photodetectors. Figure 14 illustrates of an optical response of  $80 \text{ mW cm}^{-2}$  light pulse recorded by photodetectors. The lifetime was estimated by using the following equation (John et al. 1979):

$$\tau = \left( \frac{2kT}{q} \right) \left[ \frac{1}{dV_{OC}/dt} \right] \quad (4)$$

The calculated lifetime of  $\text{In}_2\text{S}_3/\text{Si}$  photodetector increased from 14 to 22  $\mu\text{s}$  after increasing the molar concentration of  $\text{In}_2\text{S}_3$  film from 0.1 to 0.2 M; indicating an

**Fig. 15** UV pulses recorded by In<sub>2</sub>S<sub>3</sub>/Si photodetectors without external bias



improvement of photovoltaic characteristics of heterojunction photodetectors. Figure 15 illustrates a train of pulses recorded by the fabricated photodetectors after illumination with UV source in absence of external bias voltage. Pulsed responsivity of  $250 \text{ mV W}^{-1}$  was recorded for UV pulses by a photodetector prepared with 0.2 M, while the photodetector prepared with 0.1 M has a pulsed responsivity of  $200 \text{ mV W}^{-1}$ . The detector's figures of merit were investigated after three months of storing in normal ambient and no significant degradation in these parameters was observed.

## 4 Conclusion

High sensitivity n-In<sub>2</sub>S<sub>3</sub>/p-Si heterojunction photodetectors were successfully fabricated by depositing of nanostructured In<sub>2</sub>S<sub>3</sub> film on silicon using inexpensive chemical spray pyrolysis technique. The effect of film molarity on electrical characteristics and figures of merit of photodetectors was investigated. The photodetector made with 0.2 M exhibited better performance than those prepared at 0.1 M. The photoresponse measurements showed that the photodetectors have two peaks of response located at 400 nm and 750 nm indicating visible enhanced photodetectors. The maximum responsivity and detectivity of photodetectors were  $0.68 \text{ A W}^{-1}$  and  $2.5 \times 10^{11} \text{ W}^{-1} \text{ cm Hz}^{0.5}$  respectively. The results show high stability photodetectors and confirm the successful technique used for fabricating low cost visible-enhanced In<sub>2</sub>S<sub>3</sub>/Si photodetectors.

## References

- Asikainen, T., Ritala, M., Leskela, M.: Growth of InS thin films by atomic layer epitaxy. *Appl. Surf. Sci.* **82**(83), 122–125 (1994)
- El Shazly, A., Abd Elhady, D., Metwally, H., Seyam, M.: Electrical properties of thin films. *J. Phys. Condens. Matter* **10**, 5943–5954 (1998)
- Gopinath, G., Miles, R., Reddy, K.: Influence of bath temperature on the properties of In<sub>2</sub>S<sub>3</sub> films grown by chemical bath deposition. *Energy Proc.* **34**, 399–406 (2013)
- Hariskos, D., Ruckh, M., Rühle, U., Walter, T., Schock, H., Hedström, J., Stolt, L.: A novel cadmium free buffer layer for Cu (In, Ga) Se<sub>2</sub> based solar cells. *Sol. Energy Mater. Sol. Cells* **41**(42), 345–353 (1996)
- Hsiao, Y., Lu, C., Ji, L., Meen, T., Chen, Y., Chi, H.: Characterization of photovoltaics with In<sub>2</sub>S<sub>3</sub> nano-flakes/p-Si heterojunction. *Nanoscale Res. Lett.* **9**, 32–39 (2014)
- Ismail, R.: Fabrication and characteristics study of n-Bi<sub>2</sub>O<sub>3</sub>/n-Si heterojunction. *J. Semicond. Technol. Sci.* **6**, 119–123 (2006)
- Ismail, R., Al-Samarai, A.-M.E., Mohamed, S., Ahmed, H.: Characteristics of nanostructured CdO/Si heterojunction photodetector synthesized by CBD. *Solid State Electron.* **82**, 115–121 (2013)
- John, E., Thomas, W., Robert, I., Roy, K.: Measurement of minority carrier life time in solar cells from photo-induced open circuit voltage decay. *IEEE Trans. Electron. Dev.* **26**, 733–739 (1979)
- John, T., Kartha, C., Vijayakumar, K., Abe, T., Kashiwaba, Y.: Spray pyrolyzed β-In<sub>2</sub>S<sub>3</sub> thin films: effect of postdeposition annealing. *Vacuum* **80**, 870–875 (2006)
- Kaleel, S.G., Suhail, M.H., Yasser, F.M.: Spray deposition of Cu:In<sub>2</sub>S<sub>3</sub> thin films. *Int. J. Emerg. Technol. Adv. Eng.* **4**, 613–622 (2014)
- Kim, W., Kim, C.: Optical energy gaps of β-In<sub>2</sub>S<sub>3</sub> thin films grown by spray pyrolysis. *J. Appl. Phys.* **60**, 2631–2633 (1986)
- Kraini, M., Bouguila, N., Halidou, I., Timoumi, A., Alaya, S.: Properties of In<sub>2</sub>O<sub>3</sub> films obtained by thermal oxidation of sprayed In<sub>2</sub>S<sub>3</sub>. *Mater. Sci. Semicond. Process.* **16**, 1388–1396 (2013)
- Lajnef, M., Ezzaouia, H.: Structural and optical studies of In<sub>2</sub>S<sub>3</sub> thin films prepared by sulferization of indium thin films. *Open Appl. Phys. J.* **2**, 23–26 (2009)
- Lin, P., Lin, S., Cheng, S., Ma, J., Lai, Y., Zhou, H., Jia, H.: Optical and electrical properties of Ag-doped In<sub>2</sub>S<sub>3</sub> thin films prepared by thermal evaporation. *Adv. Mater. Sci. Eng.* **4**, 37086–37090 (2014)
- Liu, S., Yuan, X., Wang, P., Chen, Z., Tang, L., Zhang, E., Zhang, C., Liu, Y., Wang, W., Liu, C., Chen, C., Zou, J., Hu, W., Xiu, F.: Controllable growth of vertical heterostructure GaTe<sub>x</sub>Se<sub>1-x</sub>/Si by molecular beam epitaxy. *ACS Nano* **9**, 8592–8598 (2015)
- Naghavi, N., Spiering, S., Powalla, M., Cavana, B., Lincot, D.: High-efficiency copper indium gallium diselenide (CIGS) solar cells with indium sulfide buffer layers deposited by atomic layer chemical vapor deposition (ALCVD). *Prog. Photovolt. Res. Appl.* **11**, 437–443 (2003)
- Sabnis, S., Bhadane, P., Kulkarni, P.: Process flow of spray pyrolysis technique. *IOSR J. Appl. Phys.* **4**, 7–11 (2013)
- Sall, T., Nafidi, A., Soucase, B., Mollar, M., Hartitti, B., Fahoume, M.: Synthesis of In<sub>2</sub>S<sub>3</sub> thin films by spray pyrolysis from precursors with different [S]/[In] ratios. *J. Semicond.* **35**, 063002 (2014)
- Streetman, B., Banerjee, S.: *Solid State Electronic Devices*, 6th edn, p. 221. Pearson Prentice Hall, Upper Saddle River (2010)
- Tauc, J., Grigorovici, R., Vancu, A.: Optical properties and electronic structure of amorphous germanium. *Phys. Status Solidi B* **15**, 627–637 (1966)
- Warrier, A., John, T., Vijayakumar, K., Kartha, C.: Structural and optical properties of indium sulfide thin films prepared by silar technique. *Open Condens. Matter Phys. J.* **2**, 9–14 (2009)
- Yoshida, T., Yamaguchi, K., Toyoda, H., Akao, K., Sugiura, T., Minoura, H., Nosaka, Y.: Chemical bath deposition of band gap tailored indium sulfide thin films. *Electrochem. Soc. Proc.* **97**, 20–57 (1997)
- Yuan, X., Tang, L., Liu, S., Wang, P., Chen, Z., Zhang, C., Liu, Y., Wang, W., Zou, Y., Liu, C., Guo, N., Zou, J., Zhou, P., Hu, W., Xiu, F.: Arrayed van der Waals vertical heterostructures based on 2D GaSe grown by molecular beam epitaxy. *Nano Lett.* **15**, 3571–3577 (2015a)
- Yuan, X., Tang, L., Wang, P., Chen, Z., Zou, Y., Su, X., Zhang, C., Liu, Y., Wang, W., Liu, C., Chen, F., Zou, J., Zhou, P., Hu, W., Xiu, F.: Wafer-scale arrayed pn junctions based on few-layer epitaxial GaTe. *Nano Res.* **8**, 3332–3341 (2015b)
- Zhong, C., Luo, L., Tan, H., Geng, K.: Band gap optimization of the window layer in silicon heterojunction solar cells. *Sol. Energy* **108**, 570–575 (2014)